

# Magic-angle spinning $^{31}\text{P}$ NMR spectroscopy of condensed phosphates in parasitic protozoa: visualizing the invisible

Benjamin Moreno<sup>a</sup>, Claudia O. Rodrigues<sup>b</sup>, Brian N. Bailey<sup>b</sup>, Julio A. Urbina<sup>a,1</sup>,  
Silvia N.J. Moreno<sup>b</sup>, Roberto Docampo<sup>b</sup>, Eric Oldfield<sup>a,\*</sup>

<sup>a</sup>Departments of Chemistry and Biophysics, University of Illinois at Urbana-Champaign, 600 South Mathews Avenue, Urbana, IL 61801, USA

<sup>b</sup>Laboratory of Molecular Parasitology, Department of Pathobiology, University of Illinois at Urbana-Champaign, 2100 South Lincoln Avenue, Urbana, IL 61802, USA

Received 9 April 2002; revised 24 May 2002; accepted 10 June 2002

First published online 25 June 2002

Edited by Thomas L. James

**Abstract** We report the results of a solid-state  $^{31}\text{P}$  nuclear magnetic resonance (NMR) spectroscopic investigation of the acidocalcisome organelles from *Trypanosoma brucei* (bloodstream form), *Trypanosoma cruzi* and *Leishmania major* (insect forms). The spectra are characterized by a broad envelope of spinning sidebands having isotropic chemical shifts at  $\sim 0$ ,  $-7$  and  $-21$  ppm. These resonances are assigned to orthophosphate, terminal ( $\alpha$ ) phosphates of polyphosphates and bridging ( $\beta$ ) phosphates of polyphosphates, respectively. The average polyphosphate chain length is  $\sim 3.3$  phosphates. Similar results were obtained with whole *L. major* promastigotes.  $^{31}\text{P}$  NMR spectra of living *L. major* promastigotes recorded under conventional solution NMR conditions had spectral intensities reduced with respect to solution-state NMR spectra of acid extracts, consistent with the invisibility of the solid-state phosphates. These results show that all three parasites contain large stores of condensed phosphates which can be visualized by using magic-angle spinning NMR techniques. © 2002 Published by Elsevier Science B.V. on behalf of the Federation of European Biochemical Societies.

**Key words:** Trypanosome; Acidocalcisome; Polyphosphate; Solid state; Nuclear magnetic resonance

## 1. Introduction

Many protozoa causing human disease contain a divalent cation and phosphorus-rich organelle, the acidocalcisome, which has been implicated as: (1) an energy store in the form of phosphoanhydride bonds of polyphosphate, (2) a store for calcium for use in intracellular signaling, (3) a mechanism for the regulation of intracellular pH, and (4) a mechanism for osmoregulation [1]. Physical investigations using electron microscopy [2–4], X-ray microprobe analysis [2,3] and nuclear magnetic resonance (NMR) [5,6] have indicated that acidocalcisomes are dense vacuoles containing high levels of magnesium, calcium, sodium, zinc and phosphorus, and that the phosphorus is present as polyphosphate, with an average chain length of  $\sim 3.3$  phosphates. In addition to these

simple inorganic species, the acidocalcisome contains numerous enzymes, including a  $\text{Ca}^{2+}$ -ATPase [7,8], an  $\text{H}^{+}$ -ATPase [7,9] and an  $\text{H}^{+}$ -polyphosphatase [4,10,11].

Possession of polyphosphate granules is, however, a trait common to many other life forms. For example, *Tetrahymena pyriformis* [12], *Saccharomyces cerevisiae* [13], *Chlamydomonas reinhardtii* [14], and *Dictyostelium discoideum* [15] have all been shown to accumulate large amounts of polyphosphates and metals, and to utilize these compounds for the regulation of intracellular pH, osmotic balance and energy status by the action of polyphosphatases and phosphate transporters. In trypanosomes, acidocalcisomal transport involving  $\text{Ca}^{2+}$  and  $\text{H}^{+}$  has been well characterized biochemically [4,7–11], but until recently few studies regarding the participation of polyphosphate in these processes have appeared in the literature [16]. Given that non-parasitic organisms use polyphosphate to compensate for drastic environmental changes, it is likely that these compounds play a similar role in the lifecycle of the trypanosomes, and consequently developing methods for investigating inorganic polyphosphate metabolism in these and other systems is of interest.

As an assay for polyphosphate, solution-state  $^{31}\text{P}$  NMR is limited by the requirement for high cellular concentrations, and the inability to detect polyphosphates in high molecular weight aggregates or metal complexes, due to extensive line-broadening [17]. Fortunately however, the parasites studied here do possess high levels of polyphosphate and may be easily cultivated in numbers large enough to give NMR signal-to-noise ratios sufficient for rapid data acquisition. Most of the condensed phosphates are located in the acidocalcisomes, which may be isolated intact [18] and, as we show here, subjected to solid-state magic-angle spinning (MAS) NMR investigation. MAS NMR of semi-solids has the unique advantage of permitting the detection and characterization of immobilized polyphosphates, while completely avoiding the difficulties associated with chemical extraction.

## 2. Materials and methods

### 2.1. Culture methods

*Trypanosoma brucei* bloodstream forms (monomorphic strain 427 from clone MITat 1.4, otherwise known as variant 117) were isolated from infected mice or rats as described previously [19]. *Trypanosoma cruzi* Y strain epimastigotes were maintained at 28°C in liver infusion tryptose medium [20] supplemented with 5% heat-inactivated fetal bovine serum, 100 U/ml penicillin, 100 µg/ml streptomycin, and 20 µg/ml hemin. *Leishmania major* promastigotes (WR-205 strain)

\*Corresponding author. Fax: (1)-217-244 0997.

E-mail address: eo@chad.scs.uiuc.edu (E. Oldfield).

<sup>1</sup> Howard Hughes International Research Scholar. Permanent address: Instituto Venezolano de Investigaciones Científicas (IVIC), Caracas, Venezuela.

were grown at 28°C in medium SDM-79 [21] supplemented with 10% heat-inactivated fetal calf serum.

## 2.2. Preparation of acidocalcisomes

Acidocalcisomes were isolated as previously described [18]. For solid-state NMR, the acidocalcisomal pellet (~20 mg wet weight) was packed into a liquid sample MAS rotor insert (Doty Scientific Instruments, Columbia, SC, USA) with acidocalcisomal buffer, at 4°C. There was no loss of buffer during MAS NMR, as determined gravimetrically.

## 2.3. Chemicals

$\text{Na}_4\text{P}_2\text{O}_7$ ,  $\text{Mg}_2\text{P}_2\text{O}_7$ ,  $\text{Ca}_2\text{P}_2\text{O}_7$ ,  $\text{K}_4\text{P}_2\text{O}_7$ ,  $\text{Na}_5\text{P}_3\text{O}_{10}$ , sodium phosphate glass and sodium trimetaphosphate ( $\text{Na}_3\text{P}_3\text{O}_9$ ) were all obtained from Sigma (St. Louis, MO, USA) and were used as received.  $\text{Na}_2\text{Mg}_2\text{P}_3\text{O}_{10}\text{Cl}\cdot\text{H}_2\text{O}$  and  $\text{Na}_2\text{Ca}_2\text{P}_3\text{O}_{10}\text{Cl}\cdot\text{H}_2\text{O}$  were prepared by precipitation from 5 ml 30 mM  $\text{Na}_5\text{P}_3\text{O}_{10}$  using 6 mmol  $\text{MgCl}_2$  or  $\text{CaCl}_2$ , then filtered and dried. Elemental analysis for  $\text{Na}_2\text{Mg}_2\text{P}_3\text{O}_{10}\text{Cl}\cdot\text{H}_2\text{O}$ : Na: 11.47%, Mg: 12.12% and P: 23.17% (calculated), and Na: 10.82%, Mg: 11.34% and P: 25.76% (found). Elemental analysis for  $\text{Na}_2\text{Ca}_2\text{P}_3\text{O}_{10}\text{Cl}\cdot\text{H}_2\text{O}$ : Na: 10.63%, Ca: 18.53% and P: 21.48% (calculated), and Na: 9.69%, Ca: 18.17% and P: 23.23% (found).

## 2.4. NMR spectroscopy

Solid-state  $^{31}\text{P}$  MAS NMR spectra were acquired at 242.8 MHz using a Bruker (Madison, WI, USA) AMX600 console, a 14.1 T Oxford Instruments (Eynsham, UK) 54 mm bore magnet and a 5 mm Doty Scientific (Columbia, SC, USA) high speed MAS probe. 128 transients, 4  $\mu\text{s}$  pulse excitation, a 500 kHz spectral width, 8k data points, a 30 s recycle time and spinning speeds from 6 to 9 kHz were typically used. Solution-state  $^{31}\text{P}$  NMR spectra were acquired at 303.6 MHz using a Varian (Palo Alto, CA, USA) INOVA NMR spectrometer equipped with a 17.6 T Oxford Instruments 54 mm bore magnet using 64 (in vivo) or 1024 (extract) transients, 23  $\mu\text{s}$  (90°) pulse excitation, a 20 kHz spectral width, 32k data points, and a 10 s recycle time. All spectra were recorded  $^1\text{H}$ -coupled except for the perchloric acid extract. All in vivo spectra were obtained at 4°C to limit parasite metabolism during data acquisition. Approximately 3 g (wet weight) *L. major* promastigotes were suspended in an equal volume (~6 ml total volume) of buffer A (116 mM NaCl, 5.4 mM KCl, 0.8 mM

$\text{MgSO}_4$ , and 50 mM HEPES, pH 7.2) mixed with  $\text{D}_2\text{O}$  (10% v/v) to provide a field lock signal. The specific assignments of the in vivo resonances were based on published chemical shifts [22–24], and by correlation with established perchloric acid extract shifts [6]. Both solution and solid-state NMR spectra were referenced with respect to an 85% external phosphoric acid reference at 0 ppm, using the convention that high frequency, low field, paramagnetic or deshielded values are positive (IUPAC  $\delta$  scale). The chemical shifts of some in vivo  $^{31}\text{P}$  NMR spectra were also confirmed using a pH-independent triethylphosphate standard at 0 ppm [25].  $T_1$  determinations using the inversion recovery method indicated that all solution-state resonances were fully relaxed under the experimental conditions used. Processing of NMR spectra was performed using the Xwinnmr (Bruker, Madison, WI, USA) and VNMR (Varian, Palo Alto, CA, USA) software packages, and typically included baseline correction and 100 Hz (solid-state), 10 Hz (in vivo), or 3 Hz (extract) exponential line broadening prior to Fourier transformation. Chemical shift tensor elements were obtained using the Herzfeld–Berger method [26] employing spinning-sideband intensities deconvoluted from spectra acquired at four spinning speeds (6, 7, 8 and 9 kHz).

## 3. Results and discussion

We show in Fig. 1A–D the 242.8 MHz  $^{31}\text{P}$  MAS NMR spectra at four spinning speeds of intact acidocalcisomes isolated from *T. cruzi* epimastigotes, and in Fig. 1E–H we show similar spectra obtained from the model compound, disodium dicalcium tripolyphosphate ( $\text{Na}_2\text{Ca}_2\text{P}_3\text{O}_{10}\text{Cl}\cdot\text{H}_2\text{O}$ ). In Fig. 1A–D isotropic shifts ( $\delta_{\text{iso}}$ ) at ~0 (I), ~−7 (II) and ~−21 ppm (III) are detectable, and as indicated by the vertical lines, their chemical shifts are independent of spinning speed. Also indicated in these spectra are the  $n=−1$  sidebands of the isotropic resonances II and III, which have a separation from the isotropic resonance equal to the spinning speed. Resonance I, lacking a significant chemical shift anisotropy and encompassing the shift range from ~4 to −2 ppm, can be readily assigned to inorganic phosphate and headgroup

Table 1  
Chemical shift tensor parameters of trypanosomatid acidocalcisomes and model compounds

System	$\delta_{11}$ (ppm)	$\delta_{22}$ (ppm)	$\delta_{33}$ (ppm)	$\delta_{\text{iso}}$ (ppm)	$\Omega$	$\kappa$	Ref.
$\text{Na}_4\text{P}_2\text{O}_7$	81	−28	−46	2.3	127	−0.24	this work, [27]
$\text{K}_4\text{P}_2\text{O}_7$	82	−43	−43	−1	125	−0.34	[28]
$\text{Ca}_2\text{P}_2\text{O}_7$	76	−31	−72	−8.9	148	−0.15	this work, [27]
$\text{Mg}_2\text{P}_2\text{O}_7$	74	−21	−71	−5.9	145	−0.10	this work
$\text{Na}_5\text{P}_3\text{O}_{10}$							this work, [29]
$\alpha$	93	−37	−40	5.1	133	−0.32	
$\beta$	63	−32	−111	−5.2	174	0.21	
$\text{K}_5\text{P}_3\text{O}_{10}$							[28]
$\alpha$	113	−37	−62	5	175	−0.24	
$\beta$	79	22	−118	−6	197	0.14	
$\text{Na}_2\text{Ca}_2\text{P}_3\text{O}_{10}\text{Cl}$							this work
$\alpha$	75	−37	−62	−8.0	137	−0.21	
$\beta$	72	8	−137	−18.8	209	0.13	
$\text{Na}_2\text{Mg}_2\text{P}_3\text{O}_{10}\text{Cl}$							this work
$\alpha$	78	−33	−62	−6.0	140	−0.19	
$\beta$	65	21	−141	−18.6	206	0.19	
$\text{Na}_3\text{P}_3\text{O}_9$ (cyclic)	82	34	−169	−17.7	251	0.21	this work, [27]
Na polyP ( $n \approx 75$ )	83	23	−178	−24	261	0.18	this work, [28]
<i>T. cruzi</i> acidocalcisomes							this work
$\alpha$	104	−34	−92	−7.3	196	−0.14	
$\beta$	112	−16	−161	−21.4	273	0.02	
<i>T. brucei</i> acidocalcisomes							this work
$\alpha$	75	−34	−64	−7.7	139	−0.19	
$\beta$	51	10	−123	−20.5	174	0.17	
<i>L. major</i> acidocalcisomes							this work
$\alpha$	100	−34	−85	−6.4	185	−0.15	
$\beta$	105	−13	−158	−22.3	263	0.04	

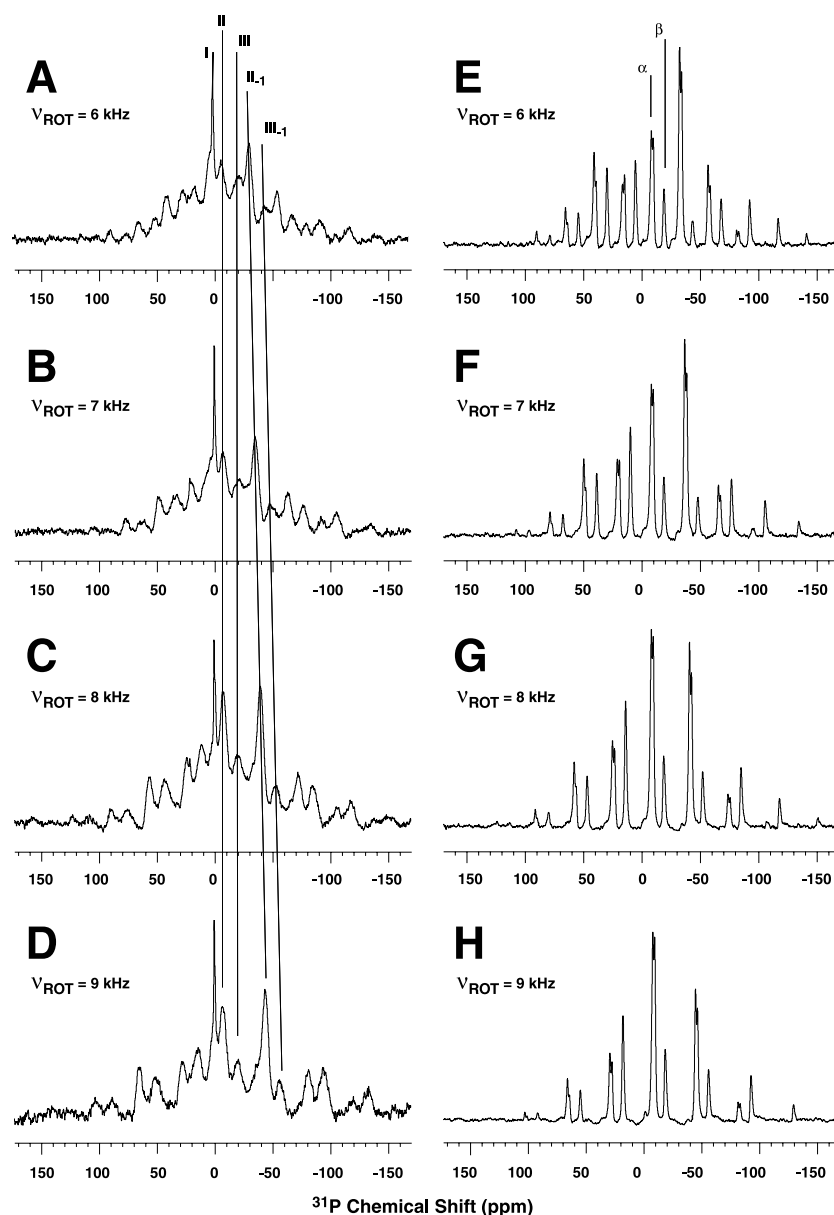


Fig. 1. 242.8 MHz  $^{31}\text{P}$  NMR spectra of (A–D) intact acidocalcisomes isolated from *T. cruzi* epimastigotes, and (E–H) the model compound  $\text{Na}_2\text{Ca}_2\text{P}_3\text{O}_{10}\text{Cl}\cdot\text{H}_2\text{O}$ . All spectra resulted from the accumulation of 512 (A–D) or 64 (E–H) free induction decays using 8  $\mu\text{s}$  pulse excitation, a 30 s recycle delay, 500 kHz spectral width, 8k data points and 6, 7, 8 or 9 kHz MAS. The FIDs were zero-filled twice and apodized with 100 Hz exponential line broadening prior to Fourier transformation. Resonance assignments are given in the text.

phosphates of acidocalcisomal membrane lipids [22]. The spinning sidebands of resonances II and III permit a determination of the chemical shift tensor elements ( $\delta_{11}$ ,  $\delta_{22}$  and  $\delta_{33}$ ) as well as the span ( $\Omega = \delta_{11} - \delta_{33}$ ) and the skew ( $\kappa = (\delta_{22} - \delta_{\text{iso}})/\Omega$ ) of these resonances in the acidocalcisomes, as shown in Fig. 1A–D for *T. cruzi*, and as shown by the representative results in Fig. 2 for *T. brucei* and *L. major*. The values obtained are given in Table 1, together with additional chemical shift tensor parameters obtained for a series of condensed phosphate model compounds [27–29].

Resonance II in the acidocalcisomes displayed an isotropic chemical shift in a region characteristic of pyrophosphate, a significant spectral span,  $\Omega$  (196, 139 and 185 ppm for *T. cruzi*, *T. brucei* and *L. major*, respectively), and negative skew values. From these spectral characteristics, resonance II can be assigned to (terminal)  $\alpha$ -phosphates of polyphosphates, in-

cluding pyrophosphate. X-ray microanalysis studies of acidocalcisomes from *L. major* and *T. cruzi* have shown that the former contain relatively more potassium and less calcium, with approximately equal levels of sodium, magnesium and phosphorus [2,3]. Isotropic  $^{31}\text{P}$  NMR chemical shifts of polyphosphate model compounds containing a single counter-ion (Table 1) show that shielding increases in the order sodium (2.3 ppm), potassium (–1 ppm), magnesium (–5.3 ppm), calcium (–8.9 ppm). Thus, the less shielded value (–6.4 ppm) obtained with the *L. major* acidocalcisomes when compared with the *T. cruzi* acidocalcisomes (–7.3 ppm) is in accord with the previously reported cation distributions in these organelles.

Resonance III, having isotropic shifts in the –21 ppm region, a large span (273, 174 and 263 ppm for *T. cruzi*, *T. brucei* and *L. major*, respectively) and a positive skew, can be as-

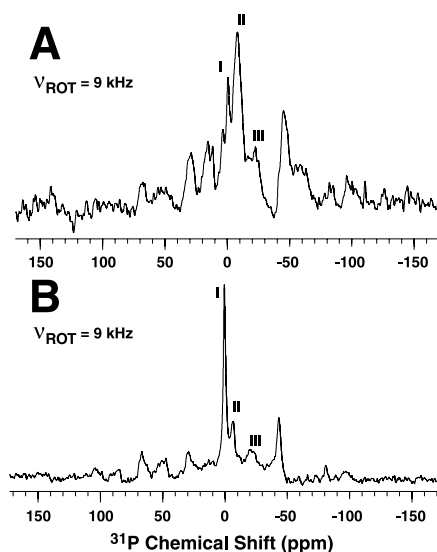


Fig. 2. 242.8 MHz  $^{31}\text{P}$  NMR spectra of intact acidocalcisomes isolated from (A) *T. brucei* bloodstream forms and (B) *L. major* promastigotes. Spectra resulted from the accumulation of 512 free induction decays using 8  $\mu\text{s}$  pulse excitation, a 30 s recycle delay, 500 kHz spectral width, 8k data points and 9 kHz MAS. The FIDs were zero-filled twice and apodized with 300 Hz (A) or 100 Hz (B) exponential line broadening prior to Fourier transformation. Resonance assignments are given in the text.

signed to the  $\beta$ -phosphates of polyphosphate. The chemical shift tensor parameters (Table 1) for both the  $\alpha$  (II) and  $\beta$  (III) resonances of the acidocalcisomes from all three species are in generally good agreement with the tensor elements found in pyro- and triphosphates complexed with magnesium or calcium, the most predominant divalent cations present in these organelles.

The integrated intensities of the  $\alpha$  and  $\beta$  resonances (and their associated sidebands) in the acidocalcisome spectra permit the calculation of the average chain length of the condensed phosphates, as follows:

$$n_{\text{ave}} = \text{P groups (mol)/polyphosphate chains (mol)} = p/m$$

$$p = \text{P groups (mol)} = \alpha \text{ P groups (mol)} + \beta \text{ P groups (mol)} = \alpha + \beta$$

$$m = \text{polyphosphate chains (mol)} = \alpha \text{ P groups (mol)}/2$$

$$n_{\text{ave}} = 2(1 + \beta/\alpha) \approx 2(1 + [\text{III}]/[\text{II}]).$$

The experimentally measured intensity ratio of  $\beta$  (III) to  $\alpha$  (II) NMR resonances was used to deduce the molar ratio of  $\beta$  to  $\alpha$  phosphate groups, yielding  $n_{\text{ave}}$ . For *T. cruzi*, *T. brucei* and *L. major*,  $n_{\text{ave}} = 3.59$ , 3.05 and 3.45, respectively, and these observations are in good agreement with previously determined average chain length values determined by solution-state NMR spectroscopy of perchloric acid extracts of isolated acidocalcisomes [6], where  $n_{\text{ave}}$  varied in the range 3.11–3.25.

Ruiz et al. found 54.3 mM levels of short-chain polyphosphates (less than 50 phosphate residues) and 2.9 mM levels of long chain polyphosphates (700–800 phosphate residues) in *T. cruzi* epimastigotes [16]. As mentioned above, the solid-state NMR spectra reveal the predominance of  $\alpha$  phosphates, indicating that the 'short-chain' class of polyphosphates reported by Ruiz et al. must be dominated by tripolyphosphate and tetrapolyphosphate. The very long-chain polyphosphates were not specifically detected in this work, due to their very low abundance.

To determine whether solid-state condensed phosphates are also present in vivo, whole, living *L. major* promastigotes were investigated by MAS NMR and a typical result is shown in Fig. 3A. The same isotropic shifts were found in this experiment as with the isolated acidocalcisomes and consequently the same resonance assignments can be made. One exception is that resonance I also contains phosphomonoester compounds (related to whole cell metabolism) which are not present in the isolated organelle. Of course, when compared with the *L. major* acidocalcisome spectrum shown in Fig. 2B, the signal-to-noise ratio of the condensed phosphate resonances in whole cells is greatly decreased due to the fact that most condensed phosphates are present in the acidocalcisomes, which only make up a small fraction of the total cell volume. Nevertheless, spinning sidebands are detectable, indicating an unaveraged chemical shift anisotropy and hence the presence of solid-state condensed phosphates in vivo.

To further investigate the nature of polyphosphates in vivo, we next obtained solution-state  $^{31}\text{P}$  NMR spectra (at 303.6 MHz) of living *L. major* promastigotes suspended in buffer A at 4°C, using conventional high resolution NMR techniques (Fig. 3B). Resonance assignments for this spectrum were made by comparison with in vivo  $^{31}\text{P}$  NMR chemical shifts in the literature [23,24], as well as with established chemical shifts of perchloric acid extracts of *L. major* promastigotes [6]. Proceeding upfield, the assignments are as follows: A, phosphomonoester compounds (predominantly phosphoethanolamine and phosphocholine); B, inorganic phosphate; C, glycerophosphocholine; D, phosphoarginine; E, terminal phosphate resonances of nucleotide phosphates as well as inorganic condensed phosphates; F,  $\alpha$  resonances of nucleotide phosphates and NADH; and G, bridging phosphates of nucleotide triphosphates and condensed inorganic phosphates. These same resonances were identified in perchloric acid extracts of the same cells (Fig. 3C, acquired in the presence of 10 mM EDTA), with the exception that the resonances from the  $\alpha$  and  $\beta$  phosphate groups of polyphosphate (E and G) are much more sharp and intense in these spectra than in those of intact cells. The insets in Fig. 3B,C illustrate the integrated intensities (expressed as a percentage of the total spectral integral) for each resonance, and clearly demonstrate that relatively little of the in vivo (Fig. 3B)  $^{31}\text{P}$  NMR spectral intensity can be attributed to polyphosphate resonances. This is, however, readily explained by the motionally restricted nature of these compounds, which leaves the substantial  $^{31}\text{P}$  chemical shift anisotropy unaveraged, resulting in (powder pattern) line widths on the order of 50 kHz, which are not detectable under normal high resolution conditions.

Magic-angle sample spinning techniques therefore enable the visualization of these otherwise invisible  $^{31}\text{P}$  NMR resonances, opening up new possibilities for in vivo NMR investigations of phosphate metabolism in parasitic protozoa, and potentially in other organisms as well.

**Acknowledgements:** We thank Linda Brown and Jim Mulligan for technical assistance. This work was supported in part by grants from the National Institutes of Health (GM-50694 to E.O. and AI-23259 to R.D.), and the United Nations Development Program/World Bank/World Health Organization Special Programme for Research and Training in Tropical Diseases (to J.A.U., R.D. and E.O.), and the American Heart Association, Midwest Affiliate (Grant 0151138Z to E.O.). B.M. was supported by an Illinois Minority Graduate Incentive Program Fellowship. B.N.B. was supported by a Student Fellowship from the American Heart Association, Midwest Affiliate.

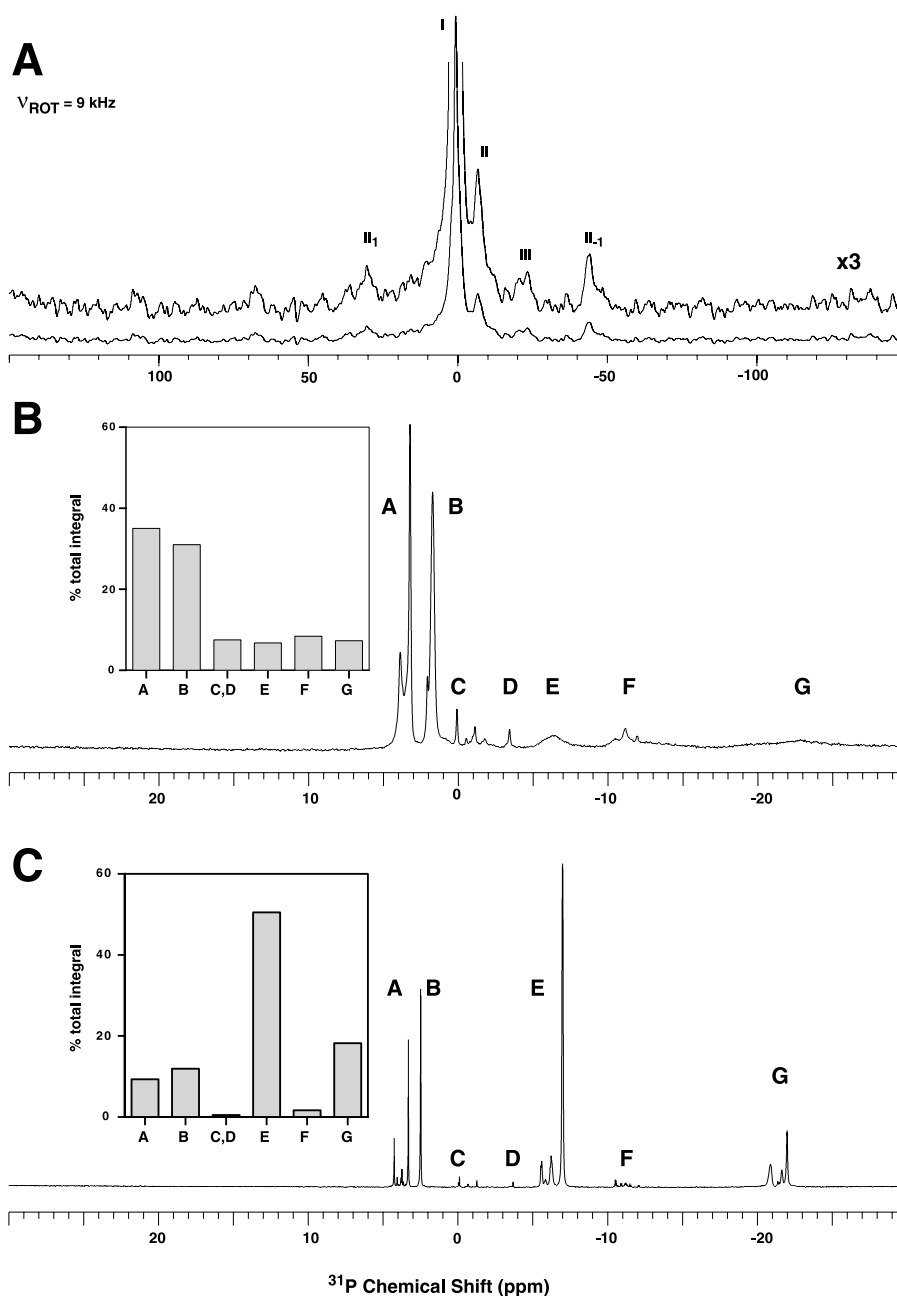


Fig. 3.  $^{31}\text{P}$  NMR spectra of *L. major* promastigotes. Spectrum A was acquired at 25°C with 9 kHz MAS and other parameters as given for Fig. 1. For the spectrum in B, promastigotes were suspended in buffer A plus 10%  $\text{D}_2\text{O}$ , and observed at 4°C by 303.6 MHz solution-state  $^{31}\text{P}$  NMR. The spectrum resulted from the accumulation of 128 free induction decays acquired with 23  $\mu\text{s}$  ( $90^\circ$ ) pulse excitation, a 10 s recycle delay, a 20 kHz spectral width and 16k data points. The perchloric acid extract spectrum shown in C was prepared from the sample in B, and was acquired similarly, except that 1024 transients were accumulated. The percentage of the total integrated intensity of each assigned peak or group of peaks are represented in the insets in B and C. The FIDs were zero-filled once and apodized with 100 Hz (A), 10 Hz (B) or 3 Hz (C) exponential line broadening prior to Fourier transformation. Resonance assignments are given in the text.

## References

- [1] Docampo, R. and Moreno, S.N.J. (1999) *Parasitol. Today* 15, 443–448.
- [2] Scott, D.A., Docampo, R., Dvorak, J.A., Shi, S. and Leapman, R.D. (1997) *J. Biol. Chem.* 272, 28020–28029.
- [3] LeFurgey, A., Ingram, P. and Blum, J.J. (1990) *Mol. Biochem. Parasitol.* 40, 77–86.
- [4] Rodrigues, C.O., Scott, D.A. and Docampo, R. (1999) *Biochem. J.* 340, 759–766.
- [5] Urbina, J.A., Moreno, B., Vierkotter, S., Oldfield, E., Payares, G., Sanoja, C., Bailey, B.N., Yan, W., Scott, D.A., Moreno, S.N.J. and Docampo, R. (1999) *J. Biol. Chem.* 274, 33609–33615.
- [6] Moreno, B., Urbina, J.A., Oldfield, E., Bailey, B.A., Rodrigues, C.O. and Docampo, R. (2000) *J. Biol. Chem.* 275, 28356–28362.
- [7] Vercesi, A.E., Moreno, S.N.J. and Docampo, R. (1994) *Biochem. J.* 304, 227–233.
- [8] Scott, D.A., Moreno, S.N.J. and Docampo, R. (1995) *Biochem. J.* 310, 789–794.
- [9] Docampo, R., Scott, D.A., Vercesi, A.E. and Moreno, S.N. (1995) *Biochem. J.* 310, 1005–1012.
- [10] Scott, D.A., de Souza, W., Benchimol, M., Zhong, L., Lu, H.G., Moreno, S.N. and Docampo, R. (1998) *J. Biol. Chem.* 273, 22151–22158.

- [11] Rodrigues, C.O., Scott, D.A. and Docampo, R. (1999) *Mol. Cell. Biol.* 19, 7712–7723.
- [12] Deslauriers, R., Ekiel, I., Byrd, R.A., Jarrell, H.C. and Smith, I.C.P. (1982) *Biochim. Biophys. Acta* 720, 329–337.
- [13] Castrol, C.D., Koretsky, A.P. and Domach, M.M. (1999) *Bio-technol. Prog.* 15, 65–73.
- [14] Ruiz, F.A., Marchesini, N., Seufferheld, M., Govindjee and Docampo, R. (2001) *J. Biol. Chem.* 276, 46196–46203.
- [15] Marchesini, N., Ruiz, F.A., Viera, M. and Docampo, R. (2002) *J. Biol. Chem.* 271, 8146–8153.
- [16] Ruiz, F.A., Rodrigues, C.O. and Docampo, R. (2001) *J. Biol. Chem.* 276, 26114–26121.
- [17] Kornberg, A. (1995) *J. Bacteriol.* 177, 491–496.
- [18] Scott, D.A. and Docampo, R. (2000) *J. Biol. Chem.* 275, 24215–24221.
- [19] Cross, G.A.M. (1975) *Parasitology* 71, 393–417.
- [20] Bone, G.J. and Steinert, M. (1956) *Nature* 178, 308–309.
- [21] Brun, R. and Schöenberg, M. (1979) *Acta Trop.* 36, 289–292.
- [22] van Wazer, J.R. and Ditchfield, R. (1987) in: *Phosphorus NMR in Biology* (Burt, C.T., Ed.), pp. 1–23, CRC Press, Boca Raton, FL.
- [23] Glonek, T. and Kopp, S.J. (1985) *Magn. Reson. Imag.* 3, 359–376.
- [24] Cholli, A.L., Yamane, T. and Jelinski, L.W. (1985) *Proc. Natl. Acad. Sci. USA* 82, 391–395.
- [25] Kozma, T.G., Omana, F., Ducoff, H.S. and Dawson, M.J. (1995) *Int. J. Hyperthermia* 11, 647–662.
- [26] Herzfeld, J. and Berger, A.E. (1980) *J. Chem. Phys.* 73, 6021–6030.
- [27] Un, S. and Klein, M.P. (1989) *J. Am. Chem. Soc.* 111, 5119–5124.
- [28] Duncan, T.M. and Douglass, D.C. (1984) *Chem. Phys.* 87, 339–349.
- [29] Burlinson, N.E., Dunell, B.A. and Ripmeester, J.A. (1986) *J. Magn. Reson.* 67, 217–230.